

Giant Zeeman splitting of light holes in GaAs/AlGaAs quantum wells

M.V. Durnev, M.M. Glazov, E.L. Ivchenko
Ioffe Physical-Technical Institute, RAS, 194021 St.-Petersburg, Russia

We have developed a theory of the longitudinal g factor of light holes in semiconductor quantum wells. It is shown that the absolute value of the light-hole g -factor can strongly exceed its value in the bulk and, moreover, the dependence of the Zeeman splitting on magnetic field becomes non-linear in relatively low fields. These effects are determined by the proximity of the ground light-hole subband, $lh1$, to the first excited heavy-hole subband, $hh2$, in GaAs/AlGaAs-type structures. The particular calculations are performed in the framework of Luttinger Hamiltonian taking into account both the magnetic field-induced mixing of $lh1$ and $hh2$ states and the mixing of these states at heterointerfaces, the latter caused by chemical bonds anisotropy. A theory of magneto-induced reflection and transmission of light through the quantum wells for the light-hole-to-electron absorption edge is also presented.

I. INTRODUCTION

The gyromagnetic ratio or g -factor determines the splitting of spin sublevels in the external magnetic field and it is one of the key parameters describing energy spectrum of charge carriers in semiconductors. It is well known that the electron and hole g -factors in bulk semiconductors differ considerably from the free electron g -factor value [1]. This difference is caused by the spin-orbit interaction and $\mathbf{k} \cdot \mathbf{p}$ mixing of the electron bands. In quantum well (QW) structures the size quantization leads to an additional strong renormalization of the g -factor as shown, e.g., in Refs. [2, 3] for the conduction band electrons (see also references cited in the book [4]) and in Refs. [5, 6] for heavy holes in the valence band. As for the light hole g -factor in QW structures, the detailed calculations were carried out only for the in-plane components $g_{xx} = g_{yy}$ (lateral or transversal Zeeman effect) [7]. The Zeeman effect on two-dimensional light hole excitons in the magnetic field directed along the structure growth axis z was studied in Refs. [8–11]. However, no microscopic calculations of the longitudinal g -factor component g_{zz} were carried out. The present theoretical work concerns the effect of quantum confinement on the longitudinal hole g -factor in the lowest light-hole subband $lh1$. It is shown below that this g -factor component is determined to a great extent by the proximity of the valence heavy-hole ($hh2$) and light hole ($lh1$) subbands and their interface mixing.

Let us recall that, in zinc-blende lattice semiconductors, the Bloch states at the valence band top transform according to four-dimensional spinor representation Γ_8 of the T_d symmetry point group. Under symmetry operations, the corresponding basis functions transform similarly to the spinor spherical harmonics $\mathcal{Y}_{Jm}^{(l)}$ with the total angular momentum $J = 3/2$ and the orbital angular momentum $l = 1$ ($m = -3/2, -1/2, 1/2, 3/2$). The Zeeman interaction of a bulk hole with the magnetic field \mathbf{B} is described by the 4×4 matrix operator [12]

$$\mathcal{H}_0 = -2\mu_B[\kappa(\mathbf{J} \cdot \mathbf{B}) + q(J_x^3 B_x + J_y^3 B_y + J_z^3 B_z)]. \quad (1)$$

Here we use the coordinate frame $x||[100]$, $y||[010]$,

$z||[001]$, $\mathbf{J} = (J_x, J_y, J_z)$ is the vector composed of the angular momentum $J = 3/2$ matrices, μ_B is Bohr magneton, κ and q are the band structure parameters. In what follows the small contribution proportional to the constant q and responsible for the anisotropic Zeeman splitting is disregarded [13]. The constant κ is related to the dimensionless Luttinger parameters γ_i ($i = 1, 2, 3$) [14, 15]. For instance, in GaAs crystals, $\kappa = 1.2$.

A uniaxial strain of the bulk crystal results in the splitting of the heavy- and light-hole Γ -point states, with angular momentum projections $\pm 3/2$ and $\pm 1/2$ onto the deformation axis. In accordance with Eq. (1) the Zeeman splittings of these states amount to $-6\kappa\mu_B B$ and $-2\kappa\mu_B B$, respectively. Hence, the light holes are described by an effective g -factor of $g_{\text{eff}} = -2\kappa$. In GaAs/AlGaAs QW structures grown along $[001]$ direction, the states of the heavy (hh) and light (lh) holes at the Γ -point, i.e., the states with zero lateral wave vector, are quantized independently and two series of quantum-confined hole states are formed: $hh\nu$ and $lh\nu$ ($\nu = 1, 2, \dots$). Here we will demonstrate that the g -factor of light holes $lh1$ strongly differs from the above value -2κ , where κ is averaged over the hole wave-function distribution between QW and barrier layers. The origin of the giant renormalization of $g_{\text{eff}}(lh1)$ is related to the fact that, in GaAs/Al_xGa_{1-x}As-type QWs, at the Γ point the $lh1$ and $hh2$ subbands are very close in energy. These subbands are intermixed owing to off-diagonal elements $H = \sqrt{3}\hbar^2\gamma_3\hat{k}_z(k_x - ik_y)/m_0$ and H^* of the Luttinger Hamiltonian [4], where m_0 is the free electron mass, γ_3 is one of the Luttinger parameters, $\hat{k}_z = -i\partial/\partial z$, and k_x, k_y are the components of the in-plane wave vector $\mathbf{k}_{||}$. Indeed, in a magnetic field applied along the z axis, the vector $\mathbf{k}_{||}$ acquires a contribution $-(e\mathbf{A}/c\hbar)$ that is proportional to the vector potential \mathbf{A} of magnetic field \mathbf{B} . The allowance for this contribution results in the mixing of the states $lh1$ and $hh2$. In the second order of the $\mathbf{k} \cdot \mathbf{p}$ perturbation theory we obtain for the effective light hole g -factor:

$$g_{\text{eff}}(lh1) = \frac{E_{lh1,1/2}(B_z) - E_{lh1,-1/2}(B_z)}{\mu_B B_z} = \quad (2)$$

$$= -2\kappa + 12 \frac{\hbar^2}{m_0} \frac{\left| \langle hh2 | \gamma_3 \hat{k}_z | lh1 \rangle \right|^2}{E_{hh2} - E_{lh1}},$$

where $|lh1\rangle$ and $|hh2\rangle$ are the hole wavefunctions describing their size quantization along z -axis, E_{lh1} and E_{hh2} are the size-quantization energies of the states $lh1$ and $hh2$ in QWs at $\mathbf{k}_{\parallel} = 0$ (in the hole representation the energies E_{lh1}, E_{hh2} are positive). It is worth to note that, in contrast to the studied geometry $\mathbf{B} \parallel z$, the magnetic field applied in the QW plane can be described by the vector potential $\mathbf{A} = (B_y z, -B_x z, 0)$ linear in z . In this case, the component H of Luttinger Hamiltonian is invariant under the mirror reflection $z \rightarrow -z$. Therefore, in symmetric wells the states $lh1$ and $hh2$ are not mixed by the in-plane magnetic field and the resonant contribution to the lateral g -factor is absent.

In the limiting case of the infinite barriers one has

$$E_{lh1} = \frac{\hbar^2 \pi^2}{2m_0 a^2} (\gamma_1 + 2\gamma_2), \quad E_{hh2} = \frac{4\hbar^2 \pi^2}{2m_0 a^2} (\gamma_1 - 2\gamma_2),$$

where a is the well width, and the matrix element in Eq. (2) is given by

$$\langle hh2 | \gamma_3 \hat{k}_z | lh1 \rangle = \frac{8i\gamma_3}{3a}.$$

An analogous expression where κ is replaced by 3κ and the second term is taken with the reversed sign describes the effective g -factor of the heavy hole in the subband $hh2$. The formula (2) can be easily extended for calculation of the g -factor in the heavy-hole $hh1$ subband in hybrid deformed QWs studied recently in Ref. [16] where the states $lh1$ and $hh1$ can be resonant. In this case, the matrix element $\langle hh1 | \gamma_3 \hat{k}_z | lh1 \rangle$ is non-zero due to the structure asymmetry as well as to an external electric field applied along the growth axis.

Following Ref. [9] we introduce an effective mass of the light hole $lh1$, which, in the resonant approximation of the $\mathbf{k} \cdot \mathbf{p}$ perturbation theory, can be presented as

$$\frac{m_0}{m_{lh1}} = \gamma_1 - \gamma_2 + 6 \frac{\hbar^2}{m_0} \frac{\left| \langle hh2 | \gamma_3 \hat{k}_z | lh1 \rangle \right|^2}{E_{lh1} - E_{hh2}}. \quad (3)$$

Comparing Eqs. (2) and (3), we obtain the relation between the g -factor and the effective mass

$$g_{\text{eff}}(lh1) = 2 \left(-\kappa + \gamma_1 - \gamma_2 - \frac{m_0}{m_{lh1}} \right).$$

This expression differs from the analogous relation, see Eq. (6) in Ref. [9], by the sign of κ .

It follows from Eq. (2) that, for the infinite barriers, the dependence of the g -factor on the QW width vanishes and is given by

$$g_{\text{eff}}(lh1) = -2\kappa - \frac{512}{3\pi^2} \frac{\gamma_3^2}{10\gamma_2 - 3\gamma_1} \approx -26. \quad (4)$$

The estimate is valid in the spherical approximation where $\gamma_2 = \gamma_3 = \bar{\gamma}$ (see Table I for the parameter values). Thus, indeed, the proximity of the ground light and excited heavy hole subbands results in a giant enhancement of the light-hole Zeeman splitting. A similar enhancement effect for the \mathbf{k} -linear spin-dependent terms in the light hole Hamiltonian was predicted by Rashba and Sherman [17].

It is instructive to analyze the effect of all heavy hole subbands on the light-hole g -factor enhancement. In the limit of infinite barriers the summation over all even subbands can be carried out analytically with the result

$$g_{\text{eff}}(lh1) = \quad (5)$$

$$-2\kappa - 12 \frac{\gamma_3^2(\nu + 1)}{\gamma_1(\nu - 1)} \left[1 + \frac{4\sqrt{\nu}}{\nu - 1} \frac{\cot \frac{\pi}{2} \sqrt{\nu}}{\pi} \right] \approx -24.7,$$

where $\nu = (\gamma_1 + 2\gamma_2)/(\gamma_1 - 2\gamma_2)$.

To conclude the introduction, we would like to point out that in real systems the absolute values and even the sign of effective g -factor may be extremely sensitive to the barrier height and QW width. Moreover, for large magnitudes of $|g_{\text{eff}}|$, the Zeeman splitting becomes non-linear function of the field, even in moderate magnetic fields. These effects are also addressed below.

II. ALLOWANCE FOR THE INTERFACE HEAVY-LIGHT-HOLE MIXING

Low C_{2v} point symmetry of the ideal (001) interface allows for the light-heavy hole mixing even at $\mathbf{k}_{\parallel} = 0$ [18, 19]. In the well with symmetric interfaces the corresponding contribution to the effective Hamiltonian can be written as [4, 18–20]

$$\mathcal{H}_{l-h} = \pm \frac{t_{l-h} \hbar^2}{\sqrt{3} m_0 a_0} \{J_x J_y\} \delta(z - z_i), \quad (6)$$

where a_0 is the lattice constant, t_{l-h} is the dimensionless mixing parameter of the order of unity, $\{J_x J_y\} = (J_x J_y + J_y J_x)/2$ is the symmetrized product of the angular momentum operators, z_i are the coordinates of interfaces. Hereafter we consider only the $lh1$ and $hh2$ hole states, assuming that the energy gap between them as well as their Zeeman splittings much smaller than the energy distance to other quantized energy states.

Figure 1() shows the results of calculation of the heavy ($hh2$) and light ($lh1$) hole energy dependence on the GaAs/ $\text{Al}_{0.3}\text{Ga}_{0.7}\text{As}$ QW width. The parameters used in calculation are summarized in Table I. In the applied spherical model, the values of γ_2 and γ_3 are replaced by the average $\bar{\gamma} = (2\gamma_2 + 3\gamma_3)/5$. Solid lines represent the energies calculated disregarding the interface mixing, i.e., at $t_{l-h} = 0$ in which case the $lh1$ and $hh2$ energy branches cross each other at the well width $a_{\text{cr}} \approx 70$ Å. Dashed lines show the calculation performed including the interface mixing effect (with $t_{l-h} = 0.5$) which results in

anticrossing of the $lh1$ and $hh2$ subbands and formation of the hybrid states

$$\Psi_{\pm 1/2}^+ = C_l^+ |lh1, \pm 1/2\rangle \pm C_h^+ |hh2, \mp 3/2\rangle, \quad (7)$$

$$\Psi_{\pm 1/2}^- = C_l^- |lh1, \pm 1/2\rangle \pm C_h^- |hh2, \mp 3/2\rangle.$$

Here the complex coefficients C_h^-, C_l^- and C_h^+, C_l^+ are interrelated by the orthogonality condition, in particular, $|C_l^+|^2 = |C_h^-|^2$ and $|C_l^-|^2 = |C_h^+|^2$; the superscript “+” or “-” in $\Psi_{\pm 1/2}^\pm$ denotes the upper and lower states with energies $E^+ > E^-$, respectively; the subscript $\pm 1/2$ enumerates degenerate states, it coincides with the projection of the angular momentum of the light-hole state admixed to $\Psi_{\pm 1/2}^+$ or $\Psi_{\pm 1/2}^-$. The energies E^\pm of mixed states and the coefficients in (7) are determined in accordance with the procedure developed in [20].

At the Γ point, the $hh2 \rightarrow e1$ optical transitions are forbidden and $lh1 \rightarrow e1$ transitions are allowed. It is therefore convenient to define g -factors of the $\Psi_{\pm 1/2}^+$ and $\Psi_{\pm 1/2}^-$ states as follows

$$g_{\text{eff}}^\pm = \frac{E_{1/2}^\pm(B_z) - E_{-1/2}^\pm(B_z)}{\mu_B B_z}. \quad (8)$$

The g -factors defined in such a way are given by

$$g_{\text{eff}}^{(+)} = -2\kappa(|C_l^+|^2 - 3|C_h^+|^2) - \Delta g_{\text{eff}}, \quad (9)$$

$$g_{\text{eff}}^{(-)} = -2\kappa(|C_l^-|^2 - 3|C_h^-|^2) + \Delta g_{\text{eff}},$$

where $\pm \Delta g_{\text{eff}}$ are the contributions to the Zeeman effect due to the magnetic field induced mixing of the split states $\Psi_{\pm 1/2}^+$ and $\Psi_{\pm 1/2}^-$ with

$$\Delta g_{\text{eff}} = 12 \frac{\hbar^2}{m_0} \frac{|\langle hh2 | \gamma_3 \hat{k}_z | lh1 \rangle|^2}{E^+ - E^-}. \quad (10)$$

This formula differs from the corresponding contribution in Eq. (2) by the replacement of the denominator $E_{hh2} - E_{lh1}$ by $E^+ - E^-$, if $E_{hh2} < E_{lh1}$, and by $-(E^+ - E^-)$, if $E_{hh2} > E_{lh1}$. Hence, far from the anticrossing point a_{cr} , Eq. (9) for $g_{\text{eff}}^{(-)}$ at $a < a_{\text{cr}}$ and that for $g_{\text{eff}}^{(+)}$ at $a > a_{\text{cr}}$ transform into Eq. (2). We note that the allowance for the penetration of hole wavefunctions into barriers results in a more complicated expression for the first term in the right-hand side of Eq. (9) representing the “bulk” contribution to the Zeeman effect. The estimations however show that this difference is negligible. The negative sign in front of $3|C_h^+|^2$ and $3|C_h^-|^2$ takes into account the state $|lh1, \pm 1/2\rangle$ mixes with $|hh2, \mp 3/2\rangle$. The interface mixing leads to an existence of gap between the energies E^+ and E^- independently of the width of the structure and finite g -factor values, even within the second order of perturbation theory. Therefore, the allowance for the interface mixing effects in the hybrid deformed structures [16] should lead to finite values of g -factors of the heavy and light holes for any value of the electric field.

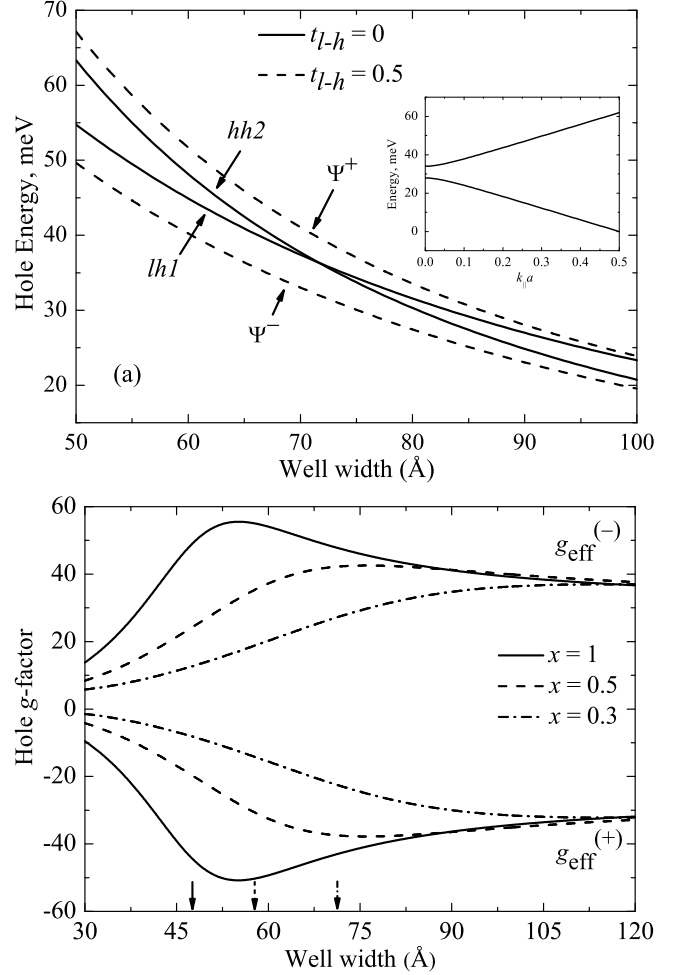


FIG. 1. (a) Heavy ($hh2$) and light ($lh1$) hole energy as a function of the GaAs/ $\text{Al}_{0.3}\text{Ga}_{0.7}\text{As}$ QW width calculated for the two values of the interface mixing parameter: $t_{l-h} = 0$ (solid lines) and $t_{l-h} = 0.5$ (dash lines). Inset shows energy dispersion of the hole subbands for the well width $a = 80$ Å. (b) The g -factors $g_{\text{eff}}^{(\pm)}$ of the split energy states E^+ and E^- as functions of QW width for three compositions x and the mixing parameter $t_{l-h} = 0.5$. Vertical arrows indicate values of the anticrossing points a_{cr} for each x .

Figure 1(b) demonstrates the calculated values of $g_{\text{eff}}^{(+)}$ and $g_{\text{eff}}^{(-)}$ as functions of GaAs/ $\text{Al}_x\text{Ga}_{1-x}\text{As}$ QW width for different contents x of Al in the barriers. It is clear that the magnetic-field induced light-heavy hole mixing results in a strong increase of the absolute value of g -factor as compared to the bulk material. One can also see that the absolute values of g -factor increase with increasing x which is a consequence of the rising barrier height. In wide wells $g_{\text{eff}}^{(+)}$ tends to its asymptotic value given by Eq. (4) because in this limiting case the wavefunction penetration in barriers can be neglected.

The absolute value of g -factor approaches its maximum in the vicinity of the anticrossing point of the $lh1$ and $hh2$ subbands. If we declared the mixed states (7) to be the

TABLE I. Parameters used in the calculation of light hole g -factor. In case of the alloys, the Luttinger parameters and the κ constant are obtained by a linear interpolation of the corresponding values for GaAs and AlAs [21], and the parabolic interpolation is applied to determine the valence band offsets.

| Material | γ_1 | γ_2 | γ_3 | $\bar{\gamma}$ | ΔE_v , meV | κ |
|--|------------|------------|------------|----------------|--------------------|----------|
| GaAs | 6.98 | 2.06 | 2.93 | 2.58 | — | 1.2 |
| Al _{0.3} Ga _{0.7} As | 6.01 | 1.69 | 2.48 | 2.16 | 140 | 0.87 |
| Al _{0.5} Ga _{0.5} As | 5.37 | 1.44 | 2.17 | 1.88 | 255 | 0.66 |
| AlAs | 3.76 | 0.82 | 1.42 | 1.18 | 600 | 0.12 |
| In _{0.53} Ga _{0.47} As | 3.7 | 5.42 | 6.31 | 5.95 | 354 | 4.63 |
| InP | 5 | 1.6 | 2 | 1.84 | — | 0.97 |

heavy-hole states as soon as $|C_l|^2 < |C_h|^2$ and light-hole states if $|C_l|^2 > |C_h|^2$, then at the anticrossing point the g -factors of the so-defined hole states would exhibit an abrupt discontinuity and sign reversal.

Since the g -factors (9) are governed by the difference of the unperturbed $hh2$ and $lh1$ energies which is extremely sensitive to the Luttinger parameters, even small variations of these parameters can considerably alter the dependence of g_{eff}^{\pm} on the well width.

III. RESONANT SPECTRA OF THE OPTICAL TRANSMISSION AND REFLECTION

Despite the development of the numerous techniques of the optical spectroscopy, experimental data on the g -factors of light holes in QWs are scarce. In Refs. [28, 29] the measured values of light hole g -factors are close to unity. More detailed investigation of the g -factors of light and heavy holes is performed in Refs. [9, 10] by differential magnetoabsorption and magnetotransmission techniques. For the theoretical analysis of these effects let us recall that, for a single-QW structure with one excitonic resonance taken into account, the light reflection (R) and transmission (T) coefficients can be written as

$$R = \left| r_{01} + \frac{e^{2i\theta} t_{01} t_{10} r_{QW}}{1 - r_{10} r_{QW} e^{2i\theta}} \right|^2 \approx R_0 [1 + S_0 f(x, \Phi)] \quad (11)$$

$$T = n \left| \frac{t_{01} e^{i\theta} (1 + r_{QW})}{1 - r_{10} r_{QW} e^{2i\theta}} \right|^2 \approx T_0 [1 - Q_0 h(x)] ,$$

where

$$R_0 = r_{01}^2, \quad T_0 = n |t_{01}|^2 ,$$

$$r_{01} = -r_{10} = -\frac{n-1}{n+1}, \quad t_{10} = n t_{01} = \frac{2n}{n+1} ,$$

and r_{QW} is the amplitude reflection coefficient from the QW, θ is the phase shift due to the light propagation over the distance between the external boundary “vacuum – cap layer” and the QW center,

$$S_0 = \frac{8n}{n^2 - 1} \frac{\Gamma_0}{\Gamma}, \quad Q_0 = \frac{2\Gamma_0}{\Gamma} ,$$

$$f(x, \Phi) = \frac{\sin \Phi + x \cos \Phi}{x^2 + 1}, \quad h(x) = \frac{1}{x^2 + 1} ,$$

$$x = \frac{\omega - \omega_0}{\Gamma}, \quad \Phi = 2\theta + \frac{\pi}{2} .$$

Other notations are common: n is the refraction index (we neglect the difference of its values in the well and the barriers), ω_0, Γ_0 and Γ are the resonant frequency, radiative and nonradiative excitonic dampings, respectively. Note, that the parameter Γ describes, in fact, the inhomogeneous broadening. Hereafter we assume that $\Gamma_0 \ll \Gamma$ and neglect terms quadratic in r_{QW} . The transmission coefficient T is defined as the ratio of the incident radiative flux and the flux escaping through the cap layer and the QW to the semi-infinite barrier.

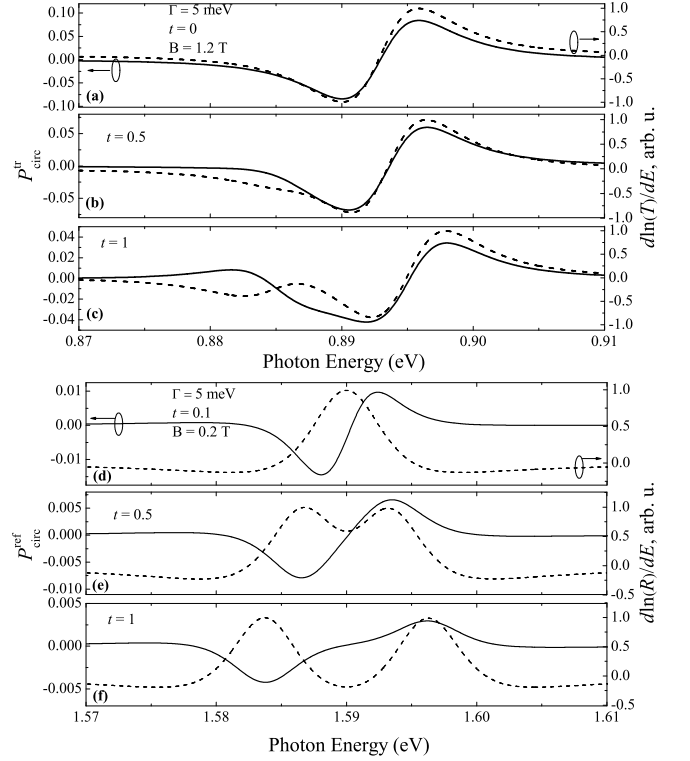


FIG. 2. (a) – (c) Transmission spectra $P_{\text{circ}}^{\text{tr}}$ (solid curves) and $d \ln T / dE$ (dashed curves) through the structure with 100 Å In_{0.53}Ga_{0.47}As/GaAs QW. The panels are computed for different strengths of heavy-light hole mixing at interfaces: $t_{l-h} = 0, 0.5$ and 1 , respectively. The nonradiative broadening $\hbar\Gamma = 5$ meV. (d) – (f) Reflection spectra $P_{\text{circ}}^{\text{ref}}$ (solid curves) and $d \ln R / dE$ (dashed curves) from the structure with 80 Å GaAs/Al_{0.36}Ga_{0.64}As QW. The panels are computed for $t_{l-h} = 0.1, 0.5$ and 1 . The nonradiative broadening $\hbar\Gamma = 5$ meV, the phase Φ is a multiple of 2π .

In Refs. [9, 10] the light-hole g -factor was experimentally determined from measurements of the differential spectra of circular magnetotransmission and magnetoreflexion defined as follows

$$P_{\text{circ}}^{\text{tr}} = \frac{T_{\sigma_+} - T_{\sigma_-}}{T_{\sigma_+} + T_{\sigma_-}}, \quad P_{\text{circ}}^{\text{ref}} = \frac{R_{\sigma_+} - R_{\sigma_-}}{R}, \quad (12)$$

where $T_{\sigma_{\pm}}$ and $R_{\sigma_{\pm}}$ are the spectrally dependent intensity coefficients of transmission and reflection of the circularly polarized light σ_{\pm} , respectively, $R = (R_{\sigma_+} + R_{\sigma_-})/2$. Replacing the resonant frequency ω_0 in Eq. (11) by the frequencies $\omega_{0,\pm} = \omega_0 \pm \Delta E/(2\hbar)$, where ΔE is the Zeeman splitting of the sublevels $lh1, 1/2$ and $lh1, -1/2$, we obtain the relationship between the differential spectra and the value of ΔE for the excitonic resonance $lh1$

$$P_{\text{circ}}^{\text{tr}} = -\frac{\Delta E}{2} \frac{d \ln T(E)}{dE} \approx -\frac{\Delta E}{2T_0} \frac{dT(E)}{dE}, \quad (13)$$

$$P_{\text{circ}}^{\text{ref}} = -\frac{\Delta E}{2} \frac{d \ln R(E)}{dE} \approx -\frac{\Delta E}{R_0} \frac{dR(E)}{dE},$$

where $E = \hbar\omega$, T_0 and R_0 are the transmission and reflection coefficients in the absence of magnetic field. We stress that these formulae are based on the assumption of a single excitonic level in the region of excitonic resonance. However, in the region of anticrossing between $e1-lh1$ and $e1-hh2$ excitons, caused by interface mixing of heavy and light holes, optical spectra are determined by two close resonances $e1-\Psi^+$ and $e1-\Psi^-$ and, strictly speaking, Eq. (13) is invalid. For this reason, we have derived an expression for the differential reflection spectra for a pair of closely-lying excitonic levels and present. The result for two resonances reads

$$R = R_0 \{1 + S_0[|C_l^+|^2 f(x_+, \Phi) + |C_l^-|^2 f(x_-, \Phi)]\}, \quad (14)$$

where $x_{\pm} = (\omega - \omega_{0,\pm})/\Gamma$. Here, for simplicity, we neglect the difference between the reduced masses of $e1-\Psi^+$ and $e1-\Psi^-$ excitons. Nonradiative decays Γ_+ and Γ_- are considered to be equal. In the presence of magnetic field one has

$$R_{\sigma_{\pm}} = R_0 \{1 + S_0[|C_l^+|^2 f(x_+ \mp \delta_+, \Phi) + |C_l^-|^2 f(x_- \mp \delta_-, \Phi)]\},$$

$$\delta_{\pm} = \frac{g_{\text{eff}}^{(\pm)} \mu_B B_z}{2\hbar\Gamma}.$$

For the differential circular reflection one obtains

$$P_{\text{circ}}^{\text{ref}} = \frac{R_{\sigma_+} - R_{\sigma_-}}{R_0} = \quad (15)$$

$$= -\frac{\mu_B B_z}{\hbar\Gamma} S_0[|C_l^+|^2 g_{\text{eff}}^{(+)} f'(x_+, \Phi) + |C_l^-|^2 g_{\text{eff}}^{(-)} f'(x_-, \Phi)],$$

$$f'(x, \Phi) = \frac{\partial f(x, \Phi)}{\partial x} = -\frac{(x^2 - 1) \cos \Phi + 2x \sin \Phi}{(x^2 + 1)^2}.$$

Let us also present the expression for the relative differential reflection in the absence of magnetic field

$$\frac{1}{R_0} \frac{dR(\hbar\omega)}{d(\hbar\omega)} = \frac{S_0}{\hbar\Gamma} [|C_l^+|^2 f'(x_+, \Phi) + |C_l^-|^2 f'(x_-, \Phi)]. \quad (16)$$

One can see that in the presence of two close resonances the ratio of $P_{\text{circ}}^{\text{ref}}$ and $d \ln R/dR$ is not a constant but rather it is a function of frequency and may even change its sign within the linewidth.

For the transmission spectra, the expressions analogous to Eqs. (15) and (16) have the form

$$P_{\text{circ}}^{\text{tr}} = \frac{T_{\sigma_+} - T_{\sigma_-}}{2T_0} = \quad (17)$$

$$= \frac{\mu_B B_z}{2\hbar\Gamma} Q_0[|C_l^+|^2 g_{\text{eff}}^{(+)} h'(x_+) + |C_l^-|^2 g_{\text{eff}}^{(-)} h'(x_-)],$$

$$\frac{1}{T_0} \frac{dT(\hbar\omega)}{d(\hbar\omega)} = -\frac{Q_0}{\hbar\Gamma} [|C_l^+|^2 h'(x_+) + |C_l^-|^2 h'(x_-)],$$

$$h'(x) = -\frac{2x}{(x^2 + 1)^2}.$$

Figure 2 presents spectra of the differential circular transmission $P_{\text{circ}}^{\text{tr}}$, panels (a)–(c), and reflection $P_{\text{circ}}^{\text{ref}}$, panels (d)–(f), calculated following Eqs. (17) and (15), respectively. The parameters of calculations are given in the figure caption. The reflectivity is calculated for the system studied in the work [10] while the transmissivity is calculated for the system studied in the work [9]. For comparison, the dashed lines show the spectra of $d \ln R/dE$ and $d \ln T/dE$ calculated from Eqs. (16) and formula in Eq. (17). Let us emphasize that in the single-resonance model the solid and dashed curves would be geometrically similar. In the InGaAs/GaAs structure [9], the heavy-hole $hh2$ and light-hole $lh1$ states are rather distant in energy. Therefore, for moderate values of the interface mixing parameter $t_{l-h} \leq 0.5$, panels (a) and (b), the difference in behaviour of $P_{\text{circ}}^{\text{tr}}$ and $d \ln T/d(2E)$ is quite small. If the interface mixing is significant, then as one can see in Fig. 2(), the spectra of $P_{\text{circ}}^{\text{tr}}$ and $d \ln T/d(2E)$ calculated for $t_{l-h} = 1$ have different qualitative behaviour.

A particularly interesting situation is realized if the $lh1$ and $hh2$ states are close in energy. This case is illustrated in Fig. 3(d)–(f) representing the differential reflection spectra $P_{\text{circ}}^{\text{ref}}$ calculated for the structure with a 80 Å GaAs/AlGaAs quantum well. Even at small strength of the interface mixing, $t_{l-h} = 0.1$, see panel (d), the spectral behaviours of $P_{\text{circ}}^{\text{ref}}$ and $d \ln R/dE$ are completely different. For example, let us consider the system tuned to the resonance between the bare $hh2$ and $lh1$ hole states so that $E_{hh2} = E_{lh1}$ and $|C_l^+|^2 = |C_l^-|^2$, $g_{\text{eff}}^{(+)} \approx -g_{\text{eff}}^{(-)}$. Moreover, let the system satisfy the condition $\omega_+ - \omega_- \ll \Gamma$. It follows then from Eq. (15) that in this case the $P_{\text{circ}}^{\text{ref}}$ spectrum is in fact described by the second derivative $f''(x, \Phi)$ whereas $d \ln R/dE \propto f'(x, \Phi)$.

Our estimations of the light hole g -factors noticeably exceed those extracted from the experiments [9, 10]. A detailed comparison between the developed theory and the existing experimental data is out of the scope of the

present paper because such a fitting requires the inclusion of many free parameters and the better accuracy of measurements. For a consistent description of experiments it is first of all necessary to determine the exact energy positions of $lh1$ and $hh2$ states. The $lh1$ - $hh2$ spacing is very sensitive to the well width, barrier height and Luttinger parameters which can lead to considerable variations of g_{eff} values.

IV. ZEEMAN SPLITTING AT HIGH MAGNETIC FIELDS

Giant values of the g -factor obtained in the previous section by means of the perturbation theory indicate that the Zeeman splitting of the light-hole spin sublevels can deviate from the linear dependence already at moderate magnetic fields. In this section we calculate the spin splitting beyond the linear approximation used in the derivation of Eqs. (2) and (9) but again assume the energy gap between $lh1$ and $hh2$ states and the hole spin splitting to be small as compared to the energy distances to other levels.

Neglecting the interface mixing of the hole states ($t_{l-h} = 0$), the pair of states $|hh2; 3/2\rangle$, $|lh1; 1/2\rangle$ are uncoupled from the pair $|hh2; -3/2\rangle$, $|lh1; -1/2\rangle$. In an external magnetic field the effective Hamiltonian that describes the pair states is analogous to the 2×2 Hamiltonian of an electron in a two-dimensional system with the spin-orbit splitting linear in the wavevector or to the Hamiltonian of “massive” Dirac Fermions [23, 24]. Decomposing the hole wavefunction over the eigen functions of a charged particle in the magnetic field [25–27], one obtains for the Zeeman splitting

$$\Delta E_Z = \frac{\tilde{E}}{2} - \sqrt{\frac{\tilde{E}^2}{4} + 6 \frac{\hbar^2}{m_0} \left| \langle hh2 | \gamma_3 \hat{k}_z | lh1 \rangle \right|^2 \hbar \omega_c}. \quad (18)$$

Here $\omega_c = |e|B/m_0c$ is the cyclotron frequency of a free electron in the magnetic field, and the $\tilde{E} = E_{lh1} - E_{hh2} - (\gamma_1 + 2\gamma_2)\hbar\omega_c$. Equation (18) is derived assuming that $E_{lh1} > E_{hh2}$, otherwise one should reverse the sign before the square root in Eq. (18).

It follows from Eq. (18) that the spin splitting ΔE_Z is a sublinear function of the field. Of course, in the limit of weak fields where $|g_{\text{eff}}|\mu_B B \ll |E_{lh1} - E_{hh2}|$, the splitting is proportional to B and the light-hole g -factor (18) reduces to Eq. (2). At high fields, where $|g_{\text{eff}}|\mu_B B \gtrsim |E_{lh1} - E_{hh2}|$ but $|\Delta E_Z|$ is still smaller than the distance to other hole subbands, the Zeeman splitting is proportional to \sqrt{B} . Correspondingly, the dash-dot line in Fig. 3 demonstrates a clear square-root asymptotics.

The allowance for the heavy-light mixing at interfaces stabilizes the linear variation of ΔE_Z with the magnetic field. In Fig. 3 we compare the magnetic-field dependence of the spin splitting depicted in the linear approximation (dashed) with the result of numerical calculations.

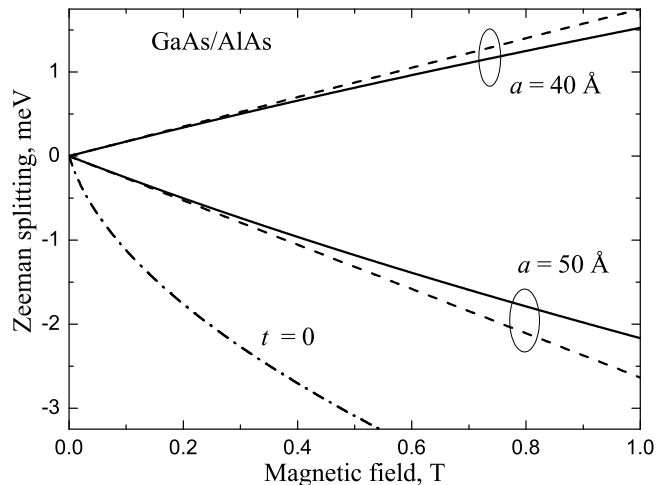


FIG. 3. Zeeman splitting of the light-hole subband $lh1$ in GaAs/AlAs QWs for two different widths: $a = 40$ Å and $a = 50$ Å. Solid lines represent numerical calculations while dashed lines represent the linear-in-magnetic-field approximation following Eq. (2). The interface hole mixing parameter $t_{l-h} = 0.5$, the size quantized energies at zero field are $E_{lh1} = 111$ meV, $E_{hh2} = 119$ meV at $a = 40$ Å and $E_{lh1} = 82.9$ meV, $E_{hh2} = 81.8$ meV at $a = 50$ Å. For comparison, dash-dot line shows the Zeeman splitting calculated from Eq. (18) in the absence of interface mixing for the particular well width $a = 50$ Å at which the $lh1$ and $hh2$ hole subbands almost touch each other at the Γ point.

tion performed beyond the this approximation. For illustration we chose two widths of the GaAs/AlAs QW, $a = 40$ Å and $a = 50$ Å. At $a = 40$ Å the light hole $lh1$ lies lower in energy than the heavy hole $hh2$ and the Zeeman splitting is positive. For $a = 50$ Å QW, the relative energy positions of the $hh2$ and $lh1$ states reverse, and the sign of Zeeman splitting changes respectively. One can see from Fig. 3 that the linear interpolation somewhat overestimates absolute values of the Zeeman splitting.

V. CONCLUSION

We have demonstrated that the proximity of the lowest light-hole ($lh1$) and first excited heavy-hole ($hh2$) subbands is responsible for a giant contribution to the Zeeman splitting of hole states. It is shown that both the magnitude and the sign of hole effective g -factor are very sensitive to the structure parameters, in particular, to the quantum well width, barrier height and heavy-light hole interface mixing parameter. We have analyzed the Zeeman splitting of light holes in a wide range of magnetic fields and derived equations for the differential magnetoabsorption and magnetotransmission spectra with allowance for the $lh1$ - $hh2$ mixing.

Authors are grateful to E.Ya. Sherman for useful discussions. This work was financially supported by RBFR,

-
- [1] L. M. Roth, B. Lax, S. Zwerdling, *Phys. Rev.* 114 (1959) 90.
 - [2] E. L. Ivchenko, A. A. Kiselev, *Fiz. Tekh. Poluprovodn.* 26 (1992) 1471 (1992) (transl: *Sov. Phys. Semicond.* 26 (1992) 827).
 - [3] I. A. Yugova, A. Greilich, D. R. Yakovlev, A. A. Kiselev, M. Bayer, V. V. Petrov, Y. K. Dolgikh, D. Reuter, A. D. Wieck, *Phys. Rev. B* 75 (2007) 245302.
 - [4] E. L. Ivchenko, *Optical Spectroscopy of Semiconductor Nanostructures*, Alpha Science Internat., Harrow, UK, 2005.
 - [5] Th. Wimbauer, K. Oettinger, A.L. Efros, B.K. Meyer, H. Brugger, *Phys. Rev. B* 50 (1994) 8889.
 - [6] A.A. Kiselev, L.V. Moiseev, *Fiz. Tverd. Tela* 38 (1996) 1574 (transl: *Phys. Solid State* 38 (1996) 866).
 - [7] A.A. Kiselev, K.W. Kim, E. Yablonovich, *Phys. Rev. B* 64 (2001) 125303.
 - [8] O. Carmel, H. Shtrikman, I. Bar-Joseph, *Phys. Rev. B* 48 (1993) 1955.
 - [9] D.M. Hofmann, K. Oettinger, A.L. Efros, B.K. Meyer, *Phys. Rev. B* 55 (1997) 9924.
 - [10] Y.H. Chen, X.L. Ye, B. Xu, Z.G. Wang, Z. Yang, *Appl. Phys. Lett.* 89 (2006) 051903.
 - [11] P. Renucci, V.G. Truong, H. Jaffrès, L. Lombez, P.H. Binh, T. Amand, J.M. George, X. Marie, *Phys. Rev. B* 82 (2010) 195317.
 - [12] G.L. Bir, G.E. Pikus, *Symmetry and strain-induced effects in semiconductors*, Nauka, Moscow, 1972; Wiley, New York, 1974.
 - [13] X. Marie, T. Amand, P. Le Jeune, M. Paillard, P. Renucci, L.E. Golub, V.D. Dymnikov, E.L. Ivchenko, *Phys. Rev. B* 60 (1999) 5811.
 - [14] J. M. Luttinger, *Phys. Rev.* 102 (1956) 1030.
 - [15] L.M. Roth, *Phys. Rev.* 133 (1964) A542.
 - [16] P. Moon, W.J. Choi, J.D. Lee, *Phys. Rev. B* 83 (2011) 165450.
 - [17] E. I. Rashba, E. Y. Sherman, *Physics Letters A* 129 (1988) 175.
 - [18] I. L. Aleiner, E. L. Ivchenko, *Pis'ma Zh. Eksp. Teor. Fiz.* 55 (1992) 662 (transl: *JETP Letters* 55 (1992) 692).
 - [19] E. Ivchenko, A. Kaminski, U. Roessler, *Phys. Rev. B* 54 (1996) 5852.
 - [20] A. A. Toropov, E. L. Ivchenko, O. Krebs, S. Cortez, P. Voisin, J. L. Gentner, *Phys. Rev. B* 63 (2001) 035302.
 - [21] I. Vurgaftman, J.R. Meyer, L.R. Ram-Mohan, *J. Appl. Phys.* 89 (2001) 5815.
 - [22] E.L. Ivchenko, P.S. Kop'ev, V.P. Kochereshko, I.N. Uraltsev, D.R. Yakovlev, S.V. Ivanov, B.Ya. Meltzer, M.A. Kaliteevskii, *Fiz. Tverd. Tela* 22 (1988) 784 (transl: *Sov. Phys. Semicond.* 22 (1988) 497).
 - [23] Y. Bychkov, E. Rashba, *J. Phys. C: Solid State* 17 (1984) 6039.
 - [24] M.Z. Hasan, C.L. Kane, *Rev. Mod. Phys.* 82 (2010) 3045; B. Buttner, C. X. Liu, G. Tkachov, E. G. Novik, C. Brune, H. Buhmann, E. M. Hankiewicz, P. Recher, B. Trauzettel, S. C. Zhang and L.W. Molenkamp, *Nature Physics* (2011) 1914.
 - [25] E.I. Rashba, *Sov. Phys. Solid State* 2 (1964) 1874.
 - [26] E. McCann, V. I. Fal'ko, *Phys. Rev. Lett.* 96 (2006) 086805.
 - [27] N. Averkiev, M. Glazov, S. Tarasenko, *Solid State Commun.* 133 (2005) 543.
 - [28] P. Lefebvre, B. Gil, J.P. Lascaray, H. Mathieu, D. Bimberg, T. Fukunaga, H. Nakashima, *Phys. Rev. B* 37 (1988) 4171.
 - [29] O. Carmel, H. Shtrikman, I. Bar-Joseph, *Phys. Rev. B* 48 (1993) 1955.